Angewandte Chemie
Eine Zeitschrift der Gesellschaft Deutscher Chemiker

Supporting Information

Induction of a Four-Way Junction Structure in the DNA Palindromic Hexanucleotide 5′-d(CGTACG)-3′ by a Mononuclear Platinum Complex

*Vincent H. S. van Rixel, Anja Busemann, Mathijs F. Wissingh, Samantha L. Hopkins, Bianka Siewert, Corjan van de Griend, Maxime A. Siegler, Tiziano Marzo, Francesco Papi, Marta Ferraroni, Paola Gratteri, Carla Bazzicalupi, Luigi Messori, and Sylvestre Bonnet**

anie_201814532_sm_miscellaneous_information.pdf

Table of content

1.1 Synthesis and characterization

NMR spectra were recorded on a Bruker AV-500 spectrometer. Chemical shifts are indicated in ppm relative to tetramethylsilane. Mass spectra were recorded by using a positive ionization mode. The elemental ultra-trace analyses were performed with an FAST (Elemental Scientific, Omaha, Nebraska, USA), i-CAP-Q ICP-MS (Thermo Scientific, Walthem, Massachusetts, USA) MP2 peristaltic pump controlled flow 110 µl/min standardized setup. The ligand 6,6'-bis[N-(pyridyl)-1-amino]-2,2'-bipyridine (H_2bapbpy), was synthesized according to literature procedures.[1] $K_2[PtCl_4]$ and cisplatin were purchased from Sigma-Aldrich.

[Pt(H_2bapbpy)](PF_6)$_2$ (1). In a 2-necked round bottom flask K_2PtCl_4 (305 mg, 0.73 mmol) H_2bapbpy, (197 mg, 0.59 mmol), and degassed ethanol-water mixture (3 : 2; 30 mL) were added. The brown suspension was stirred 16 h at 90 ºC under argon, resulting in a red suspension. To ensure full coordination of the ligand another K_2PtCl_4 (17 mg, 0.041 mmol) was added, and the mixture was stirred for 3 more hours. Then, the suspension was cooled to room temperature, and subsequently cooled on ice. The precipitate was filtered off and the filtrate was concentrated *in vacuo*. Then, a saturated aqueous solution of KPF_6 (3.5 mL) was added to the filtrate inducing a yellow solid to precipitate. The suspension was filtered over a membrane filter, and washed with 10 mL water, 10 mL Et_2O, and 10 mL hexanes. The complex was obtained as a yellow powder and dried *in vacuo*. Yield: 209 mg (43%). *^{1}H NMR (500 MHz, DMSO-d6, 293 K, in ppm)*: δ = 12.32 (s, 2H, NH), 8.48 (dd, *J* = 8 Hz, 2H, H^4), 8.41 (d, *J* = 7.6 Hz, 2H, H^3), 8.36 (d, *J* = 6.4 Hz, 2H, $H^{py\text{-}6}$), 8.27 (dd, *J* = 8.8 Hz, 2H, $H^{py\text{-}4}$), 7.69 (d, *J* = 8 Hz, 2H, H^5), 7.62 (d, *J* = 8.4 Hz, 2H, $H^{py\text{-}3}$), 7.28 (dd, *J* = 6.8 Hz, 2H, $H^{py\text{-}5}$). *^{13}C NMR (126 MHz, DMSO-d6, 293 K, in ppm)*: δ = 152.42, 149.25, 147.19, 146.10, 141.05, 119.85, 117.76, 116.43, 116.01. *High resolution ES MS m/z (calc.)*: 534.0998 (534.1001, $[1 - 2 \times PF_6 - H]^+$). *Elem. Anal. Calcd. For $C_{20}H_{16}F_{12}N_6P_2Pt+H_2O$*: *C, 28.48; H, 2.15; N, 9.96; N, 10.23*. *Found*: C, 28.38; H, 2.37; N, 9.39.

1.2 Single Crystal X-ray crystallography for [Pt(Hbapbpy)]PF_6

Single crystals were obtained by the vapor diffusion method. In short, **1** in acetonitrile (0.5 mg/mL) was put in a small vial that was placed in a larger vial containing 2.8 mL toluene. The large vial was screw capped, taped with PTFE-tape and vapor diffusion occurred within a few days to afford good quality crystals suitable for X-ray structure determination.

All reflection intensities were measured at 110(2) K using a SuperNova diffractometer (equipped with Atlas detector) with Cu Kα radiation (λ = 1.54178 Å) for [Pt(Hbapbpy)]PF_6 under the program CrysAlisPro (Version 1.171.36.32 Agilent Technologies, 2013). The temperature of the data collection was controlled using the system Cryojet (manufactured by Oxford Instruments). The CrysAlisPro software was used to refine the cell dimensions and for data reduction. The structure was solved by direct methods with SHELXS-2014/7[2] and was refined on F^2 with SHELXL-2014/7.[2] Analytical numeric absorption correction based on a multifaceted crystal model was applied using CrysAlisPro. The H atoms were placed at calculated positions (unless otherwise specified) using the instructions AFIX 43 with isotropic displacement parameters having values 1.2 Ueq of the attached C atoms. The structure is mostly ordered except for the PF_6^- counteranion that is found disordered over two orientations. The occupancy factor of the major component of the disorder refines to 0.661(10). A

careful check for the existence of H atoms attached to N2 and N5 were performed by looking at the difference Fourier maps. The H atom on N5 could be found, and there are intermolecular N–H…F interactions. On the other hand, there is no H atom attached to N2. The N2–C distances (C5–N2 = 1.354(7), C6–N2 = 1.336(7)) are significantly shorter than the N5–C distances (C15–N5 = 1.373(8), C16–N5 = 1.398(8))

Table S1. Experimental details for the crystal structure of compound 1

	1
Crystal data	
Chemical formula	$C_{20}H_{15}N_6Pt \cdot F_6P$
M_r	679.44
Crystal system, space group	Triclinic, *P*-1
Temperature (K)	110
a, *b*, *c* (Å)	8.1311 (3), 10.6084 (3), 12.1246 (3)
α, β, γ (°)	91.338 (2), 107.313 (3), 93.775 (2)
V (Å^3)	995.28 (5)
Z	2
Radiation type	Cu *K*α
μ (mm^{-1})	14.69
Crystal size (mm)	0.25 × 0.16 × 0.03
Data collection	
Diffractometer	SuperNova, Dual, Cu at zero, Atlas
Absorption correction	Analytical *CrysAlis PRO*, Agilent Technologies, Version 1.171.36.32 (release 02-08-2013 CrysAlis171 .NET) (compiled Aug 2 2013,16:46:58) Analytical numeric absorption correction using a multifaceted crystal model based on expressions derived by R.C. Clark & J.S. Reid. (Clark, R. C. & Reid, J. S. (1995). Acta Cryst. A51, 887-897)
T_{min}, T_{max}	0.151, 0.733
No. of measured, independent and observed [$I > 2\sigma(I)$] reflections	12277, 3867, 3647
R_{int}	0.049

$(\sin \theta/\lambda)_{max}$ ($Å^{-1}$)	0.616
Refinement	
$R[F^2 > 2\sigma(F^2)]$, $wR(F^2)$, S	0.033, 0.087, 1.07
No. of reflections	3867
No. of parameters	374
No. of restraints	256
H-atom treatment	H atoms treated by a mixture of independent and constrained refinement
$\Delta\rho_{max}$, $\Delta\rho_{min}$ (e $Å^{-3}$)	0.98, -1.79

Computer programs: *CrysAlis PRO*, Agilent Technologies, Version 1.171.36.32 (release 02-08-2013 CrysAlis171 .NET) (compiled Aug 2 2013, 16:46:58), *SHELXS2014*/7,[2] *SHELXL2014*/7,[2] *SHELXTL* v6.10 (Sheldrick, 2008).

1.3 pKa determination

pH titration: 6 mL of a 67 µM solution of [Pt(H_2bapbpy)]Cl_2 in hydrochloric acid (0.033 M) was put in a 15 mL vial. A pH measurement electrode was added and when stable the pH was logged, aliquots (0.5-10 µL) of aqueous NaOH (0.05 – 5 M) were added to give a range of pH values while stirring. After each stable pH a UV-vis absorbance spectrum was measured. The relative concentration of $[Pt(H_2bapbpy)]^{2+}$ was determined using the Lambert-Beer Law, and then plotted as a function of the pH. The pKa was determined by modelling the curve using a simplified two-parameter Hill-slope equation: $\frac{100}{(1+10^{((log_{10}pka-X)\cdot Hill\ Slope)})}$.

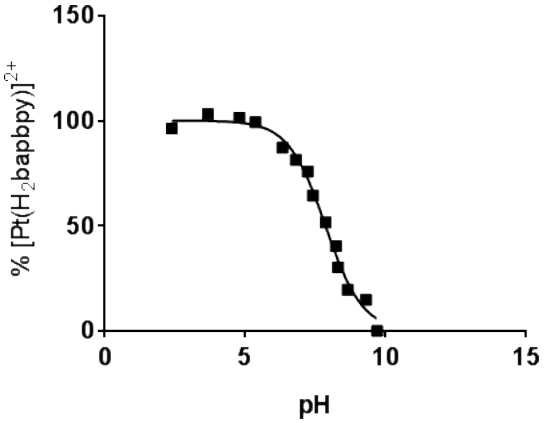

Figure S1. pH dependent presence of $[Pt(H_2bapbpy]^{2+}$ (%) at different pH in water.

1.4 Thermal stability by UV-vis spectroscopy

UV-vis experiments were performed on a Cary 50 Varian spectrometer equipped with a Cary Single Cell Peltier for temperature control. All spectra were recorded with Cary WinUV software from Cary and further processed with Microsoft Office Excel 2010. Three 100 µM solution of 1 in MilliQ water, PBS (pH=7.0), or Opti-MEM cell growing medium, were prepared and their UV-vis spectrum measured every hour for 2 days. The spectra are shown Figure S2.

In H_2O the compounds, introduced as the acidic solid $[Pt(H_2bapbpy)](PF_6)_2$, is stable under the bis-protonated form $[Pt(H_2bapbpy)]^{2+}$, and the mass spectrum at the end of the experiment shows both $[Pt(Hbapbpy)]^+$ and $[Pt(H_2bapbpy)]^{2+}$ species.

In both PBS and OptiMEM medium the spectra corresponds to the mono-protonated form $[Pt(Hbapbpy)]^+$ due to the neutral pH (the color of the solution at the same concentration is also darker for the compound in PBS than in H2O due to the different molar absorption coefficient of the bis-protonated vs. mono-protonated species). The absorption maximum did not shift over 2 days, showing that the compound did not react, but the absorption intensity did change consecutively to the formation of a thin precipitate over 3 days. The mass spectrum confirmed that only the $[Pt(Hbapbpy)]^+$ species was present in PBS after 3 days. ESI mass spectra in OptiMEM were impossible due to the sensibility of the mass spectrometer, but the UV-vis and the precipitate match that in PBS.

Overall, the data show that $[Pt(H_2bapbpy)](PF_6)_2$ is not reacting with water, PBS, or cell media, but is deprotonated in neutral buffer to form $[Pt(Hbapbpy)]PF_6$ that is less soluble and therefore precipitates to some extent, at the concentration tested.

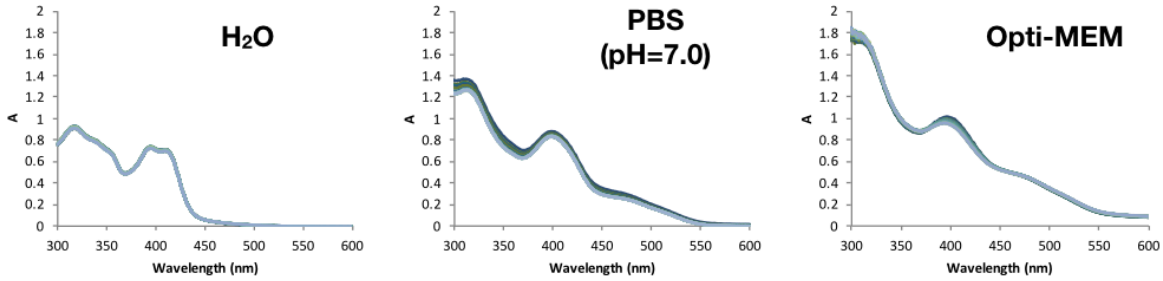

Figure S2. Evolution of UV-vis absorbance spectra of 1 (100 µM) in milliQ water, phosphate buffer saline, or cell growing media, at 37 °C, for 48 h (1 spectrum per hour).

1.5 Single crystal growing of 1-CGTACG

Crystal screenings were performed for the adducts formed by 1 with the DNA sequences 5'-CGTACG-3' and 5'-CGATCG-3'. The HPLC purified oligonucleotides were purchased from Jena Bioscience (Jena, Germany) and annealed without further purification in 10 mM Tris-sulfate, 1 mM EDTA at pH 7.2 (1 mM dsDNA final concentration). Freshly made solutions of the metal complexes in DMSO (10 mM concentration) were used to prepare solutions of the adducts at both dsDNA:complex 1:1 and 1:2 stoichiometric ratios. Crystal screenings were performed by using the sitting drop vapor diffusion method and the plates were stored in incubator at 23°C. Yellow crystals were successfully obtained after five months from a drop initially composed of 2 μL of the 1-CGTACG adduct as in 1:1 stoichiometric ratio and 2 μL of 40 mM sodium cacodylate pH 7.0, 20 mM $MgCl_2$, 80 mM $SrCl_2$, 12 mM spermine tetrachloride, 10% v/v MPD equilibrated against 100 μL of 30% v/v MPD. Crystals belong to the $P3_221$ space group with unit cell dimensions a=b=30.09, c=116.99 Å.

1.6 Structure determination of 1-DNA

Crystals were analysed at the ID-30B beam line at the ESRF synchrotron (Grenoble, France) at 100K using as cryoprotectant solution the crystallization condition with a increased concentration of precipant (25% v/v MPD). A complete collection of reflections were obtained up to 2.3 Å resolution using a wavelength of 0.97264 Å and a Dectris Pilatus3 6M detector . Data were integrated and scaled using the program XDS. Data are hemihedrally twinned (twin law -h,-k,l). The possibility of twinning was suggested by the analysis of the intensity distribution calculated using the phenix.xtriage module of the PHENIX program.[3] The crystal structure of the adduct was solved by Molecular Replacement using Phaser[4] from the CCP4 program suite.[5] The coordinates of the Berberine-CGTACG adduct (PDB accession code 3NP6)[6] were used as search model after deleting ligands, water molecules as well as metal ions. The Fo-Fc density map showed the presence of two disordered metal complexes sharing the same binding site. The model was refined using the program Refmac5[7] using 0.5 occupancy factors for each metal complexes, and taking into account twinning. Due to the relatively low resolution and the twinning issues, no attempts were done for an anisotropic treatment of the metal centers and all thermal factors were treated as isotropic. The coordinates and library for the metal complex were built by the crystal structure of $[Pt(Hbapbpy)]PF_6$. Manual rebuilding of the model was performed using the program Coot.[8] After the last cycle of refinement Rfree and Rfactors converged to a value of 0.29 and 0.26, respectively, and the twin fraction was equal to 0.18. Final coordinates and structure factors have been deposited with the Protein Data Bank (PDB accession code 6F3C).

Notations: the four crystallographically independent DNA oligomers are defined as [C1A, G2A, T3A, A4A, C5A, G6A], [C7B, G8B, T9B, A10B, C11B, G12B], [C1C, G2C, T3C, A4C, C5C, G6C] and [C7D, G8D, T9D, A10D, C11D, G12D], respectively, and represented in Figure 2 and 3 in red, blue, green, and pink colour, respectively.

*Table S2. Summary of Data Collection and Atomic Model Refinement Statistics for the **1**-CGTACG adduct. Values in parentheses are for the highest resolution shell.*

Data Collection	
Wavelength (Å)	0.97264
Space group	*P* 3_221
Cell dimension (Å)	a=30.09, c= 116.99
Limiting resolution (Å)	39.00-2.29 (2.43-2.29)
Unique reflections	3083 (469)
Rsym (%)	16.4(152.7)
Rmeas (%)	17.0(157.9)
CC1/2	99.3 (32.6)
Multiplicity	16.2 (15.0)
Completeness overall (%)	99.6 (98.5)
<I/σ(I)>	10.35 (1.09)
Refinement	
Resolution range (Å)	39.0-2.30
Unique reflections, working/free	2732/ 347
Rfactor (%)	0.257
Rfree(%)	0.292
r.m.s.d. bonds(Å)	0.020
r.m.s.d. angles (°)	1.781

*Table S3. Rotational parameters for the eight steps B-type double helix units formed by the four strands in the crystal structure of the **1**-(CGTACG)$_4$ adduct.*

Base pairs	Twist (Ω)	Propeller twist (ω)	Buckle (κ)	Roll (ρ)
G8B-C5A	0.00	-4.14	-6.81	0.00
T9B-A4A	38.14	-5.78	1.49	1.04
A10B-T3A	38.23	-6.72	-1.78	0.86
C11B-G2A	30.89	3.76	7.72	4.26
G2C-C11D	-69.26	6.56	-4.53	1.56
T3C-A10D	26.56	-3.33	-7.55	3.39
A4C-T9D	42.43	-0.17	-5.33	-0.11
C5C-G8D	27.28	-2.23	8.83	2.63

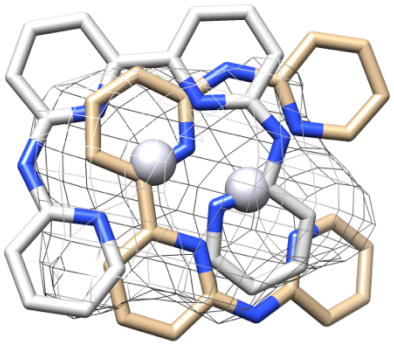

*Figure S3. Relative orientations of the platinum complex **1** in the conformations **1**-F (light gray) and **1**-G (sand) of the crystal structure of the **1**-(CGTACG)$_4$ adduct. OMIT electron density map for **1**-F and **1**-G are contoured at 2.0σ level.*

1.7 QM/MM calculations

The model for 1-CGTACG adduct was built starting from the coordinates of the crystal structure, deleting some of the residues and most of the water molecules. Moreover, two models were defined as follows, considering the two orientations found for the platinum-complex in the crystallographic binding site: 1) platinum complex F, DNA: chain A (G2, T3, A4, C5, G6); chain B (G8, T9, A10, C11); symmetry related chain B (C7; x-y, -y, 1/3-z); chain C (T3, A4, C5, G6); chain D (G8, T9, A10); symmetry related chain D (C7; x-y, -y, 1/3-z); water molecule HOH6; 2) platinum complex G, DNA: chain A (G2, T3, A4, C5, G6); chain B (G8, T9, A10, C11); symmetry related chain B (C7; x-y, -y, 1/3-z); chain C (T3, A4, C5, G6); chain D (G8, T9, A10); symmetry related chain D (C7; x-y, -y, 1/3-z); water molecules HOH10, symmetry related HOH10 (x-y, -y, 1/3-z). QM/MM calculations were performed by the Qsite software.[9] This method allowed a quantum-mechanical (QM) treatment of the metal complex and the water molecules at the DFT/B3LYP[10] level of theory with the LACVP basis set,[11] which uses an effective core potential for the metal atom, while models the DNA via a classical molecular mechanics force field (MM-OPLS2005 forcefield[12]). During all procedure, the coordinates of the platinum ions were constrained to the crystallographic positions in both the 1-F and 1-G conformation models.

Overall, *in silico* relaxation did not lead to significant variations of the conformation of the model (Figure S4 and S5), compared to that of the crystal structure. **1**-F (Figure 4a - manuscript) remained mainly in contact on the one hand with C5C and G8D, and one the other hand with G6A, G8B, and C5A, via π-π stacking at an approximate inter-planar distance of 3.2-3.3 Å, while conformation **1**-G (Figure 4b - manuscripèt) mainly gives π-stacking with residues G8B and C5A (3.3-3.4 Å), and with G6A and G8D (3.3-3.6 Å). In addition, As shown in Figure 4a, in complex **1**-F the HOH6 water molecule bridges the hydrogen atom of the secondary amine of **1** (NH···O distance 2.27 Å, N···O distance 2.82 Å) and the N3 nitrogen in residue C7-B (OH···N distance 2.27 Å, O···N distance 3.22 Å). On the other hand, the nitrogen in conformation **1**-G points toward the phosphate oxygen atom PO2 of residue G8D (insert of Figure 4b), even though with longer distances (NH···O 2.75 Å, N···O 3.78 Å). The contact N···O distances from the XRD analysis (2.6 and 3.5 Å in complex **1**-F and 4.1 Å in complex **1**-G) were too long to be sure for the presence of a H-bond interaction considering the insufficient quality of the electron density map for that level of description. However, the QM/MM model suggested that specific H-bonding interactions between DNA and the bridging non-coordinated amine bridges of the platinum-bound ligand, may play a role in the stabilization of the DNA 4WJ.

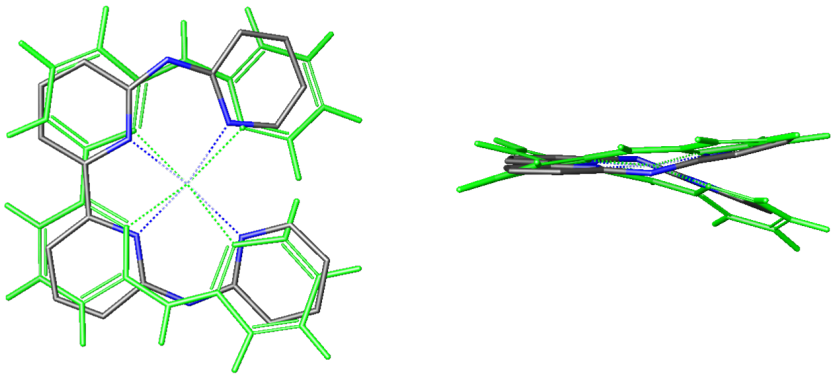

A B

*Figure S4. Conformation **1**-F from crystal structure overlapped to QM/MM calculation result (green): (A) top view, (B) lateral view.*

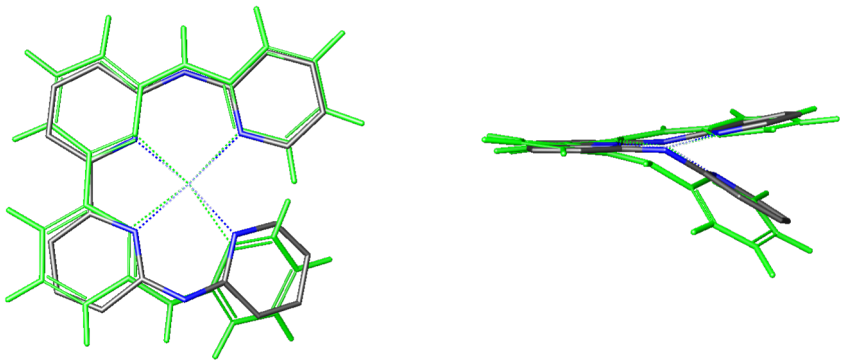

A B

*Figure S5. Conformation **1**-G from crystal structure overlapped to QM/MM calculation result (green): (A) top view, (B) lateral view.*

1.8 DNA binding studies

The pUC19 plasmid used for this study (2686 bp) exists in three forms: supercoiled (SC), single-nicked open circular (OC) and linear dimer (LD). Of particular interest are the SC and OC forms. Although these two forms have the same number of bp, the SC form migrates faster through the agarose gel than the OC form due to the condensed SC form. However, as positively charged metal complexes associate with the SC form, the shape may become larger and it will be less negatively charged, ultimately resulting in slower migration. Alternatively, if metal complexes coordinatively modify the OC form, it may induce coiling or a condensed structure causing an increase in migration and thus coalescence of the SC and OC form on increasing metal complex concentration. However, if there is no condensation of the OC plasmid structure, but the positively charged metal complexes associate with the OC form then the observed migration would be retarded.

Agarose gel electrophoresis was used to assay the binding of **1** to pUC19 plasmid DNA. Two buffers were used for the experiments: 5X tris-boric acid buffer (TBA) and phosphate buffer (PB). TBA (45 mM tris(hydroxymethyl)amino methane and 45 mM boric acid, pH = 7.4) was used in the gel and running buffer. PB (100 mM NaH_2PO_4, pH = 7.0) was used for DNA-MC interactions. The agarose gels were 0.8% w/w agarose gel (0.24 g agarose, 24 g DI H_2O, and 6 mL TBA) and were cast in the OWL B1A Easycast system.

The molar concentration of the pUC19 plasmid DNA base pairs (BP) was determined using its extinction coefficient ($\varepsilon_{260\ nm}$ = 13,200 $M^{-1}cm^{-1}$).[13] All aliquots were prepared with a final volume of 20 µL and prior to loading 4 µL of 6X loading dye was added. The λ DNA-HindIII digest molecular weight (MW) marker was prepared by adding 2 µL (1 µg) of the DNA MW marker, 18 µL PB, and 4 µL 6X loading dye. The MW marker was heated for 3 min at 60 °C prior to loading. In each well, 12 µL (1 µg of pUC19 DNA or 0.5 µg of MW marker) of each sample was loaded.

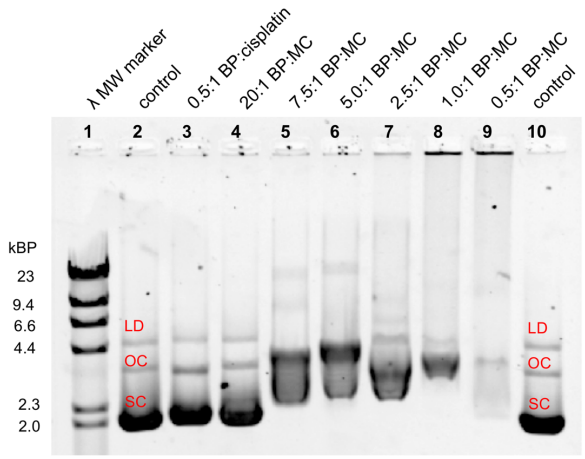

*Figure S6. Agarose gel of pUC19 plasmid DNA incubated with **1**. The lanes correspond to (1) λ DNA MW marker, (2 and 10) DNA control, (3) 0.5:1 BP:cisplatin control, (4-9) 20:1, 7.5:1, 5.0:1, 2.5:1, 1.0:1, 0.5:1 BP:MC ratio (BP = base pair, MC = metal complex). The bands of the λ MW marker correlate to 23, 9.4, 6.6, 4.4, 2.3, and 2.0 kbp. The DNA control bands are labelled according to the form the linear dimer (LD), open circular (OC), and supercoiled (SC) DNA. $t_{incubation}$ = 24 h, $T_{incubation}$ = 37 °C.*

For each gel, the electrophoresis chamber was filled with 50 mL TBA and 210 mL demineralized H_2O. Each gel was run at a constant voltage of 105 V for 90 min. All gels were stained using 10 µL

(10 mg/mL) ethidium bromide in 200 mL demineralized H_2O for 30 min with slight shaking and then destained in 200 mL demineralized H_2O for 20 min. Immediately following destaining, the gel was imaged using a BioRad ChemiDoc imaging system (ethidium bromide setting). Image Lab software was used to process the images.

The samples for thermal binding were prepared under ambient light in amber centrifuge tubes. For each sample 2 μL of pUC19 plasmid (2 μg, $[BP]_{stock} = 1.95 \times 10^{-3}$ M) was used and the amount of metal complex and PB were adjusted to a final volume of 20 μL ($[BP]_{final} = 195$ μM). Several ratios of base pairs of the plasmid (BP) to metal complex (MC) ($[MC]_{final} = 9.8$, 26, 39, 78, 195, and 391 μM, corresponding to 20:1, 7.5:1, 5.0:1, 2.5:1, 1.0:1, and 0.5:1 BP:MC ratios, respectively) were incubated at 37 °C for 24 h. Additionally, the negative control (DNA without metal complex) and a positive control (cisplatin, 391 μM, 0.5:1 BP:MC ratio) were incubated under the same conditions. Lanes were loaded as follows: **(1)** λ MW marker, **(2)** DNA only control, **(3)** cisplatin (0.5:1 BP:MC, $[cisplatin]_f$ = 390 μM) control, **(4)** M complex **1** (20:1 BP:MC, $[M]_f = 9.8$ μM), **(5)** M complex (7.5:1 BP:MC, $[M]_f$ = 26 μM), **(6)** M complex (5.0:1 BP:MC, $[M]_f = 39$ μM), **(7)** M complex (2.5:1 BP:MC, $[M]_f = 78$ μM), **(8)** M complex (1.0:1 BP:MC, $[M]_f = 195$ μM), **(9)** M complex (0.5:1 BP:MC, $[M]_f = 391$ μM), and **(10)** DNA only control. The gels were run, stained, and processed as described above.

1.9 Cell culturing

Cells were thawed and at least passaged twice before starting (photo)cytotoxicity experiments. Each cell line was cultured in Dulbecco's Modified Eagle Medium with phenol red, supplemented with 8.0% v/v fetal calf serum (FCS), 0.2% v/v penicillin/streptomycin (P/S), and 0.9% v/v Glutamine-S (GM). Cells were cultured in either 25 cm^2 or 75 cm^2 flasks and split at 70-80% confluence (three times per week for 25 cm^2 flasks, once per week for 75 cm^2 flasks). The flasks were incubated at 37 °C at 7.0% CO_2. The medium was refreshed three times a week. Cells used in all biological experiments were cultured for a maximum of eight weeks.

1.10 Cytotoxicity assay

The (photo)cytotoxicity of cancer cell lines (A549, MCF-7, and MDA-MB231) or one non-cancerous lung cell line (MRC-5) was assessed using an assay adapted from Hopkins et al.[14] Cell cultures with a maximum confluence of 70-80% were trypsinized and centrifuged (1.5 min, 1.2 relative centrifugal force), trypsin and DMEM complete were removed, and the cells were re-suspended using Opti-MEM supplemented with 2.4% v/v FCS, 0.2% v/v P/S, and 1.0% v/v GM, (hereafter called Opti-MEM complete). 10 µL of cell suspension and 10 µL of trypan blue were mixed and pipetted into a cell counting slide, and cells were counted. The cell suspension was diluted to the appropriate seeding density (A549, 5×10^3; MCF-7, 8×10^3; MDA-MB231, 12×10^3; MRC-5, 6×10^3 cells/well) and seeded in the wells of a 96-well plate. Cisplatin positive control solution was prepared from a stock solution based on clinical formulation (3.3 mM cisplatin, 55 mM mannitol, 154 mM NaCl).[15] Dimethylsulfoxide (DMSO) was used to dissolve in such amounts that the maximum v/v% of DMSO per well did not exceed 0.5% v/v%.

A complete cytotoxicity experiment lasted 96 h: cells were seeded at t = 0 h, treated at t = 24 h, the medium was refreshed at t = 48 h, and fixed at t = 96 h. The cells were incubated in the dark for 24 h at 37 °C at 7.0% CO_2. At t = 24 h the cells were treated with freshly prepared solutions of the compounds and dissolved in Opti-MEM complete. Different concentrations were prepared and of each concentration 100 µL was added to three wells. The medium was refreshed at t = 24 h and placed back into the incubator for the remainder of the experiment, until the cells were fixated by addition of 100 µL TCA (10% w/v).

The plates were stored at 4 °C for at least 4 h as part of the SRB assay that was adapted from Vichai at al.[16] In short, after fixation the TCA medium mixture was removed, rinsed with demineralized water three times, and air dried. Then, each well was stained with 100 µL SRB solution (0.6% w/v SRB in 1% v/v acetic acid) for 30 min, the SRB solution was removed, and washed with acetic acid (1% v/v) until no SRB came off, normally requiring 3-5 times. Once air dry, 200 µL of tris base (tromethamine, 10 mM) was pipetted to each well. To determine the cell viability the absorbance at 510 nm was measured using a M1000 Tecan Reader. To make sure all the SRB was dissolved, this measurement was performed at least 30 minutes after addition of tris base. The SRB absorbance data per compound per concentration was averaged over three identical wells (technical replicates, $n_t = 3$) in Excel and made suitable for use in GraphPad Prism. Relative cell populations were derived from the average of the untreated controls ($n_t = 6$). In any case, it was checked that the cell viability of the control cells of the samples irradiated without compound were similar (maximum difference of 10%) to the unirradiated samples without ruthenium compound to make sure no harm was done by the light. The data from three independent biological replications was used to obtain the dose-response curves

and EC_{50} values using non-linear regression of hills-slope equation with a fixed Y maximum (100%) and minimum (0%) relative cell population values.[14]

1.11 Cell fractionation

Cell fractionation for intracellular distribution studies for **1** and cisplatin and cisplatin were conducted on A549 lung cancer cells. 3×10^6 cells were seeded at t = 0 h in Opti-MEM complete in 175 cm^2 flasks. At t = 24 h cells were treated with complexes to give final concentrations of 1.0 and 3.3 µM for respectively **1** and cisplatin in a total volume of 24 mL. After 24 h of drug incubation at 37 °C, the medium was removed, the cells were washed with PBS-buffer, trypsinized, counted and pelleted by centrifugation (700 × g, 5 min, at room temperature). Then, the pellets were fractionated using the FractionPREP cell fractionation kit from BioVision or Mitochondria Isolation Kit for Cultured Cells from ThermoFisher according to the instruction of the supplier. Samples were digested overnight in concentrated nitric acid (> 65%) and diluted with MilliQ water to obtain a final concentration of 5% HNO_3. For ICP-MS measurements, the system was optimized with a palladium-platinum solution. The calibration range was from 0 to 25 µg/l, and obtained detection limit for all isotopes was 0.01 µg/l. Silver and indium were used for internal standard, to correct for sample dependent matrix effects. The recoveries of the spiked concentrations were all within a 10% deviation. The data from three independent biological replications.

Table S4. Uptake in the different fractions of A549 cells for compounds 1 and cisplatin.

Compound	Treatment (μM)	Metal uptake (pmol/10^6 cells)	Metal uptake efficiency (%)	Fractions	Relative Metal Distribution (%)	Metal Distribution (pmol/10^6 cells)
1	1.0	1586 ± 667	47	Cytosol	2	28.8 ± 8.5
				Membrane	35	555 ± 180
				Nucleus	15	236 ± 140
				Cytoskeleton	48	766 ± 350
Cisplatin	3.3	22.9 ± 6.1	< 0.1	Cytosol	8	1.89 ± 0.7
				Membrane	64	14.6 ± 3.1
				Nucleus	14	3.13 ± 1.1
				Cytoskeleton	14	3.28 ± 1.3

1.12 What happens in solution?

To establish whether the studied Pt complex may be able to interact with a preformed 4WJ DNA structure, we selected the sequence 5'-CCGGTACCGG-3' that under certain conditions (*A. Franklin et al. Biochemistry, 2006, 45, 2647*) is known to exist almost exclusively under the form of a 4WJ DNA structure. As compound [Pt(bapbpy)]$(PF_6)_2$ manifests a few relatively intense absorption bands in the visible/near UV (Figure S7, black trace) the time evolution of the absorption band at 410 nm upon addition of a molar excess of a DNA sample existing in a 4WJ conformation, was monitored for 24 h.

HPLC-purified 5'-CCGGTACCGG-3' oligonucleotide sequence was purchased from Metabion International AG and purified by HPLC. The complex [Pt(bapbpy)]$(PF_6)_2$ (0.1 mM) was incubated for 24 h at 20 °C with the 4WJ formed by 5'-CCGGTACCGG-3' oligonucleotide sequence (1 mM) in presence of 25 mM of sodium cacodylate buffer (pH=7) and $CaCl_2$ 150 mM. The result is shown as the red trace in Figure S7. Due to the presence of intense DNA absorptions in the UV, the spectrum after DNA addition is reliable only above 380 nm. In any case it is evident that addition of the DNA oligomer in excess in solution conditions appropriate for the formation of a 4WJ structure causes important modifications in the shape and intensity of the band that is characteristic of the Pt complex. The spectral changes are rapid and reach completion in a few seconds, to not change anymore for the next 24 h (all measured spectra after 4WJ addition were superimposable to the red trace in Figure S7). These data offer a first indication of the fact that the Pt complex is able to interact with 4WJ like DNA structures in solution.

However, this observation is only an indication and much more need to be done, in particular to demonstrate whether the changes are due to interaction with the double-stranded part of the sequence or with its 4WJ part. Still, we think that this experiment is a sign that something happens in solution as well, which we are currently studying now in more detail.

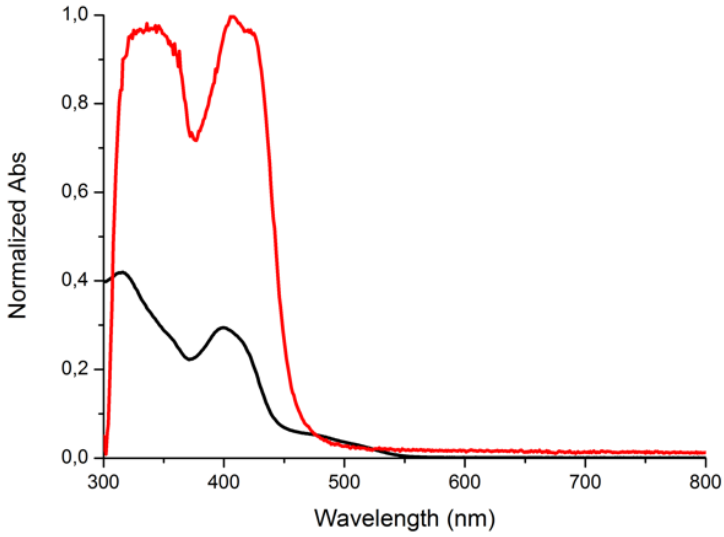

Figure S7. UV-Vis spectra of the complex [Pt(bapbpy)]$(PF_6)_2$ (0.1 mM) incubated for 24 h at 20 °C with the 4WJ formed by 5'-CCGGTACCGG-3' oligonucleotide sequence (1 mM) in presence of 25 mM of sodium cacodylate buffer (pH=7) and $CaCl_2$ (150 mM).

1.13 References

[1] S. Bonnet, G. Molnár, J. Sanchez Costa, M. A. Siegler, A. L. Spek, A. Bousseksou, W.-T. Fu, P. Gamez, J. Reedijk, *Chem. Mater.* **2009**, *21*, 1123-1136.

[2] G. M. Sheldrick, *Acta Cryst. C* **2015**, *71*, 3-8.

[3] P. D. Adams, R. W. Grosse-Kunstleve, L. W. Hung, T. R. Ioerger, A. J. McCoy, N. W. Moriarty, R. J. Read, J. C. Sacchettini, N. K. Sauter, T. C. Terwilliger, *Acta Cryst. D* **2002**, *58*, 1948-1954.

[4] A. J. McCoy, R. W. Grosse-Kunstleve, P. D. Adams, M. D. Winn, L. C. Storoni, R. J. Read, *J. Appl. Crystallogr.* **2007**, *40*, 658-674.

[5] M. D. Winn, C. C. Ballard, K. D. Cowtan, E. J. Dodson, P. Emsley, P. R. Evans, R. M. Keegan, E. B. Krissinel, A. G. W. Leslie, A. McCoy, S. J. McNicholas, G. N. Murshudov, N. S. Pannu, E. A. Potterton, H. R. Powell, R. J. Read, A. Vagin, K. S. Wilson, *Acta Cryst. D* **2011**, *67*, 235-242.

[6] M. Ferraroni, C. Bazzicalupi, A. R. Bilia, P. Gratteri, *Chem. Commun.* **2011**, *47*, 4917-4919.

[7] G. N. Murshudov, A. A. Vagin, E. J. Dodson, *Acta Cryst. D* **1997**, *53*, 240-255.

[8] P. Emsley, B. Lohkamp, W. G. Scott, K. Cowtan, *Acta Cryst. D* **2010**, *66*, 486-501.

[9] a) Schrödinger release 2017-4, New York, NY, **2017**; b) R. B. Murphy, D. M. Philipp, R. A. Friesner, *J. Comput. Chem.* **2000**, *21*, 1442-1457; c) D. M. Philipp, R. A. Friesner, *J. Comput. Chem.* **1999**, *20*, 1468-1494.

[10] a) J. C. Slater, in *Quantum theory of molecules and solids, Vol. 4*, McGraw-Hill, New York, **1974**; b) P. Hohenberg, W. Kohn, *Phys. Rev. B* **1964**, *136*, 864.

[11] P. J. Hay, W. R. Wadt, *J. Chem. Phys.* **1985**, *82*, 299-310.

[12] J. L. Banks, H. S. Beard, Y. X. Cao, A. E. Cho, W. Damm, R. Farid, A. K. Felts, T. A. Halgren, D. T. Mainz, J. R. Maple, R. Murphy, D. M. Philipp, M. P. Repasky, L. Y. Zhang, B. J. Berne, R. A. Friesner, E. Gallicchio, R. M. Levy, *J. Comput. Chem.* **2005**, *26*, 1752-1780.

[13] S. M. Zeman, D. M. Crothers, *Methods Enzymol.* **2001**, *340*, 51-68.

[14] S. L. Hopkins, B. Siewert, S. H. C. Askes, P. Veldhuizen, R. Zwier, M. Heger, S. Bonnet, *Photochem. Photobiol. Sci.* **2016**, *15*, 644-653.

[15] M. D. Hall, K. A. Telma, K.-E. Chang, T. D. Lee, J. P. Madigan, J. R. Lloyd, I. S. Goldlust, J. D. Hoeschele, M. M. Gottesman, *Cancer Res.* **2014**, *74*, 3913-3922.

[16] V. Vichai, K. Kirtikara, *Nat. Protoc.* **2006**, *1*, 1112-1116.